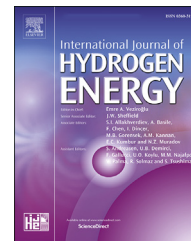


Available online at www.sciencedirect.com

ScienceDirect

journal homepage: www.elsevier.com/locate/ije

Solid metal-hydrogen solutions with a symmetric miscibility gap

Vladimir E. Antonov ^{a,b,*}, Vitaly D. Muzalevsky ^a, Nikita S. Orlov ^a

^a Institute of Solid State Physics RAS, 142432, Chernogolovka, Moscow District, Russia

^b National Research University Higher School of Economics, 20 Myasnitskaya ul., 101000 Moscow, Russia

HIGHLIGHTS

- Model of solid solutions Pd–H with a symmetric two-well mixing energy is considered.
- The model explains the linear dependence $\ln P(1/T)$ for formation of palladium hydride.
- The formation pressure is determined by the reaction $\text{Pd} + (z/2)\text{H}_2 = \text{PdH}_z$ at $z = 0.63$
- Deviation of $\ln P(1/T)$ from linearity in this approximation is 1% at $194.5 \leq T \leq 565$ K.
- Similar results are obtained for the systems Pd–D, Ni–H, and Ni–D.

ARTICLE INFO

Article history:

Received 12 January 2022

Received in revised form

2 March 2022

Accepted 3 March 2022

Available online 31 March 2022

Keywords:

Palladium-hydrogen system

Nickel-hydrogen system

Phase diagrams

Thermodynamics of solid solutions

ABSTRACT

It is shown that the T - x projection of the miscibility gap in solid interstitial MeH_z solutions will be symmetric and the pressure vs. temperature dependence of the corresponding isomorphous phase transformation will be determined by the reaction $\text{Me} + (z/2)\text{H}_2 = \text{MeH}_z$ with a fixed z value attained at $T \rightarrow 0$ K, if the mixing Gibbs energy of the solutions is a symmetric two-well function of the H content with a maximum at $z/2$. Based on these findings and using the literature data for the pure metal Me and the hydride MeH_z , it is explained why the experimental dependences of the standard Gibbs energy for the isomorphous transformation between two solid phases of variable composition in the Pd–H and Pd–D systems ($z = 0.63$) and in the Ni–H and Ni–D systems ($z = 1$) are close to linear in the entire investigated temperature range.

© 2022 Hydrogen Energy Publications LLC. Published by Elsevier Ltd. All rights reserved.

Introduction

A large number of metal-hydrogen systems exhibit a linear dependence $\ln P(1/T)$ in wide ranges of temperature (T) at low hydrogen pressures (P) where hydrogen can be considered as ideal gas for phase transformations occurring between solid

phases with different hydrogen concentrations. Formally, such a dependence could be observed for the transformation $\text{Me} + (z/2)\text{H}_2 = \text{MeH}_z$, where $z = \text{const}$, if the standard (referred to $P_0 = 1$ atm) enthalpy ΔH^0 and entropy ΔS^0 of this transformation did not depend on temperature, since in this case

* Corresponding author. Institute of Solid State Physics RAS, 142432, Chernogolovka, Moscow District, Russia.

E-mail address: antonov@issp.ac.ru (V.E. Antonov).

<https://doi.org/10.1016/j.ijhydene.2022.03.034>

0360-3199/© 2022 Hydrogen Energy Publications LLC. Published by Elsevier Ltd. All rights reserved.

$$\begin{aligned} \ln(P/P_0) &= 2/(zRT)\{G_{\text{MeHz}}^0 - G_{\text{Me}}^0 - G_{\text{H}_2}^0\} = 2/(zRT)\Delta G^0 \\ &= 2/(zR)\{\Delta H^0/T - \Delta S^0\}, \end{aligned} \quad (1)$$

where ΔG^0 is the standard Gibbs energy of transformation and R is the universal gas constant.

We were unable to find in the literature a discussion of the question of why the values of ΔH^0 and ΔS^0 for the formation of a hydride with fixed hydrogen content $H/\text{Me} = z$ are weakly temperature dependent. Instead, a more mysterious problem has been discussed for several decades: why the linear dependence $\ln P(1/T)$ is observed in the most widely used and best studied Pd–H system (see Fig. 1a), in which the hydride is formed by an isomorphous transition between phases of variable composition – depleted in hydrogen (primary solid solution) and enriched in hydrogen (hydride). The compositions of these phases approach each other with increasing temperature until they coincide at the critical point, and this can be depicted on the T - x projection of the T - P - x phase diagram as a dome of the miscibility gap in the solid Pd–H solutions (Fig. 1b).

The problem was considered in most detail in Refs. [6,7]. Both papers, however, only analyzed the behavior of $\Delta H^0(T)$ derived from the slope of $\ln P$ as a function of the reciprocal temperature. In Ref. [6], the following expression was obtained for the three-phase equilibrium $\text{Me}_{1-y}\text{H}_y + \frac{1}{2}(x-y)\text{H}_2 = \text{Me}_{1-x}\text{H}_x$:

$$\begin{aligned} \frac{d(\ln P^{1/2})}{d(1/T)} &= \frac{(1-x)(1-y)(\bar{H}_m - \bar{H}_m) + xy(\bar{H}_H - \bar{H}_H)}{(x-y)R} \\ &+ \frac{y(\bar{H}_H - \bar{H}_H) + x(\bar{H}_H - \bar{H}_H)}{(x-y)R} \end{aligned}$$

In this expression, the symbols \bar{H} denote the partial molar enthalpies of the phases participating in the reaction. The unprimed symbols refer to the primary solid solution $\text{Me}_{1-y}\text{H}_y$, the single-primed symbols to the non-stoichiometric hydride $\text{Me}_{1-x}\text{H}_x$, and the double-primed symbols to the gaseous hydrogen. The enthalpies of the primary solution and hydride are unknown functions of the temperature and hydrogen concentration. As noted in Refs. [6,7], the obtained expression is “not amenable to facile quantitative interpretation.”

In Ref. [7], the authors considered separately the equilibrium with hydrogen of single-phase solid solutions and hydrides near the transformation line. After some simplifications and assumptions, the following expression was obtained:

$$\begin{aligned} \frac{d(\ln P^{1/2})}{d(1/T)} &= \frac{\Delta H_{-H}^{\text{calc}}}{R} = \frac{\Delta \bar{H}_{-H}}{R} + T^2 \left\{ \frac{1}{n(1-n)} - 24 \left[\frac{2n\omega' - \omega' - \beta}{\beta^2 + \beta - 2n\beta} \right. \right. \\ &\left. \left. + \frac{1}{2} \left(1 - n \right) \right] + \frac{1}{RT} \left(\frac{\partial \Delta \mu_e(n)}{\partial n} \right)_T \right\} \frac{dn}{dT}, \end{aligned}$$

where $n = H/\text{Pd}$; $\beta = [1 - 4n(1-n)(1 - \exp(-\omega/RT))]^{1/2}$; $\omega' = 1 - \exp(-\omega/RT)$; ω is the pairwise interaction energy between the two hydrogen atoms, and $\Delta \mu_e(n)$ has been attributed to a filling-in of the d-band of palladium by electrons from the hydrogen atoms.

The authors of Ref. [7] came to the conclusion that the factors leading to the constancy of $d(\ln P^{1/2})/d(1/T)$ in the above equation were largely fortuitous, but they did not specify what those factors were. The authors also considered it quite possible that for systems other than Pd–H, $d(\ln P^{1/2})/d(1/T)$ may have significant temperature dependence.

At the same time, linear dependences $\ln P$ vs. $1/T$ and/or $\Delta G^0/T$ vs. $1/T$ were also observed for isomorphous transformations in the Nb–H system [8] (Fig. 2a) and the Ni–H system [9] (Fig. 3a). This is already a regularity that cannot be attributed to random coincidences. A common feature of

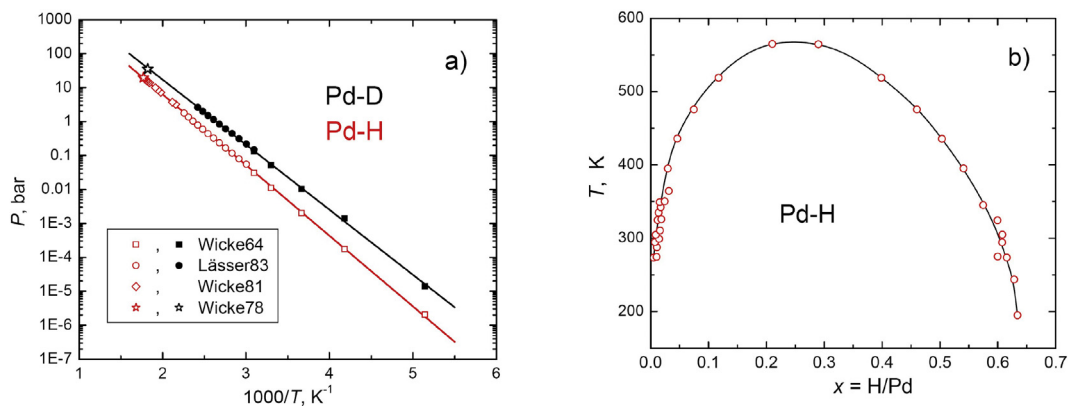


Fig. 1 – Compilation of experimental data available in the literature for the Pd–H and Pd–D systems. (a) Decomposition pressures of palladium hydrides (open red symbols) and deuterides (solid black symbols) determined in Refs. [1] (Wicke64), [2] (Lässer83), and [3] (Wicke81). The open stars show the positions of the critical point [4] (Wicke78). (b) T - x projection of the Pd–H phase diagram: the literature data compiled in Ref. [5]. (For interpretation of the references to color in this figure legend, the reader is referred to the Web version of this article.)

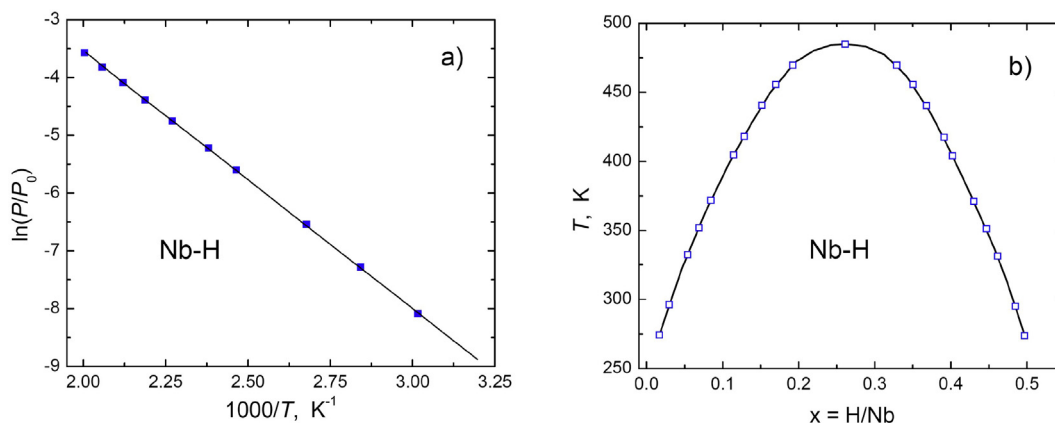


Fig. 2 – Decomposition pressures of niobium hydrides (a) and T-x projection of the phase diagram of the Nb–H system (b) determined in Ref. [8]. $P_0 = 1 \text{ bar} = 0.1 \text{ MPa}$.

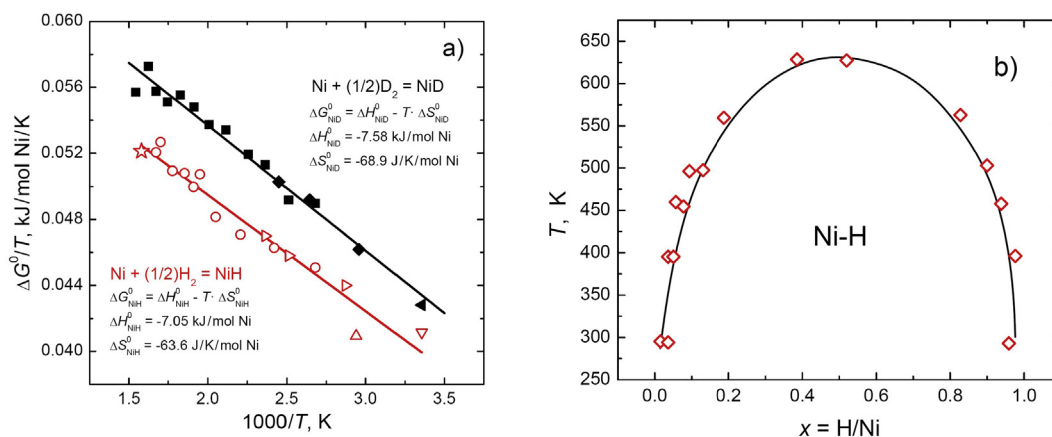


Fig. 3 – (a) Available experimental values of the standard Gibbs energy $\Delta G^0/T$ as a function of $1/T$ for the reactions $\text{Ni} + \frac{1}{2}\text{H}_2 \rightarrow \text{NiH}$ (open red symbols) and $\text{Ni} + \frac{1}{2}\text{D}_2 \rightarrow \text{NiD}$ (solid black symbols) compiled and corrected in Ref. [9]. (Phase transformations in the Ni–H and Ni–D systems occur at pressures of the order of 1 GPa when hydrogen can no longer be considered an ideal gas, therefore the $\ln P$ vs. $1/T$ dependences are substantially nonlinear.) (b) T-x projection of the phase diagram of the Ni–H system [10]. (For interpretation of the references to color in this figure legend, the reader is referred to the Web version of this article.)

all three systems Pd–H [5], Nb–H [8], and Ni–H [10] is the symmetry of the miscibility gap of the Me–H solid solutions with respect to the critical concentration $x_{cr} = z/2$, where z is the atomic ratio H/Me for the hydride phase at $T \rightarrow 0 \text{ K}$ (see Figs. 1b, 2b and 3b, respectively).

This paper proposes possible solutions to two problems:

- i) Assuming that the mixing Gibbs energy of the interstitial Me–H solid solution is a two-well function symmetric with respect to the hydrogen content $x_{cr} = z/2$, leads to a symmetric miscibility gap and shows that the temperature dependence of the pressure of the corresponding isomorphic phase transformation is determined only by the temperature dependences at a fixed pressure of $P_0 = 1 \text{ atm}$ of the thermodynamic properties of the pure metal and its hydride with the fixed composition MeH_z attained at $T \rightarrow 0 \text{ K}$.
- ii) Using the available literature data on the $P(T)$ dependences for the isomorphic phase transformation and temperature

dependences of the heat capacities of pure metal Me and hydride (deuteride) with an invariable composition MeH_z (MeD_z), gives negligible deviations from linearity for the temperature dependences of the standard Gibbs energy $\Delta G^0(T) = \Delta H^0(T) - T \cdot \Delta S^0(T)$ of transformations in the Pd–H, Pd–D, Ni–H, and Ni–D systems. The changes in $\Delta G^0(T)$ are much less than the changes in $\Delta H^0(T)$ and $T \cdot \Delta S^0(T)$, because these terms mostly have the same sign and partially compensate each other.

Thermodynamics of solid solutions with a symmetric energy of mixing

The condition for the equilibrium of two phases at a given temperature and pressure in any two-component system is the presence of a common tangent line to the concentration dependences of the Gibbs energy of these phases. If

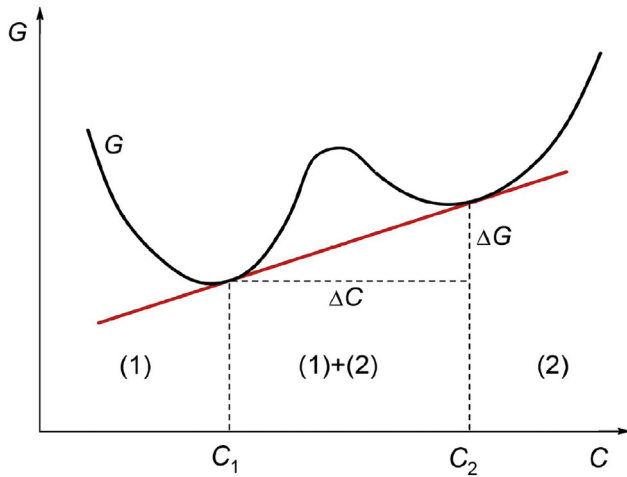


Fig. 4 – Graphical illustration of the common tangent rule for two-phase equilibrium in solid solutions.

components A and B form a solid solution, then all phases are described by one common potential $G(T, P, c)$, and the common tangent rule turns into

$$\begin{cases} \frac{\partial G}{\partial c}(c_1) = \frac{\partial G}{\partial c}(c_2) \\ \frac{\partial G}{\partial c}(c_2) = \frac{G(c_2) - G(c_1)}{c_2 - c_1} = \frac{\Delta G}{\Delta c} \end{cases} \quad (2) \text{ and } (3)$$

where c_1 and c_2 are the concentrations of component A in the two phases in equilibrium with each other [11]. The rule is illustrated in Fig. 4.

Substitutional solid solutions

Consider a substitutional solid solution with components A and B and write its Gibbs energy in the form

$$G(T, P, c) = c \cdot G_A(T, P) + (1 - c) \cdot G_B(T, P) + \Delta G_{\text{mix}}(T, P, c),$$

where G_A and G_B are the Gibbs energies of crystals of pure components, and ΔG_{mix} is the mixing energy, the sign of which determines whether the formation of solid solution is energetically favorable ($\Delta G_{\text{mix}} < 0$) or unfavorable ($\Delta G_{\text{mix}} > 0$). Now let ΔG_{mix} represent a double-well potential as a function of the concentration c at temperatures and pressures below critical, and let it be symmetric with respect to the replacement of c by $1-c$, i.e., $\Delta G_{\text{mix}}(c) = \Delta G_{\text{mix}}(1-c)$. As can easily be shown, the derivative $\partial(\Delta G_{\text{mix}})/\partial c$ should be an antisymmetric function of c , i.e., $\partial(\Delta G_{\text{mix}}(c))/\partial c = -\partial(\Delta G_{\text{mix}}(1-c))/\partial c$ (for example, introducing a new variable $t = c - 1/2$, the problem can be reduced to the well-known lemma that the derivative of an even function $G(t)$ must be odd).

To make further formulas look simpler, let $\Delta G_{\text{mix}}(c) = f(c)$ and $\partial(\Delta G_{\text{mix}}(c))/\partial c = \varphi(c)$. For fixed values of T and P , we then get

$$G(c) = c \cdot G_A + (1 - c) \cdot G_B + f(c) \quad (4)$$

$$\partial G / \partial c = (G_A - G_B) + \varphi(c) \quad (5)$$

Substitution of these expressions into conditions (2) and (3) for the existence of a common tangent line gives

$$\varphi(c_1) = \varphi(c_2) \quad (6)$$

$$\varphi(c_2) = [f(c_2) - f(c_1)] / (c_2 - c_1) \quad (7)$$

Next, replacing c_2 by $1-c_2$ in Eq. (7) and using the symmetry of $f(c)$ and antisymmetry of $\varphi(c)$ for the inverse replacement $1-c_2 \rightarrow c_2$ results in

$$\begin{aligned} \varphi(1-c_2) &= [f(1-c_2) - f(c_1)] / (1-c_2 - c_1) \\ -\varphi(c_2) &= [f(c_2) - f(c_1)] / (1-c_2 - c_1) \end{aligned} \quad (8)$$

Adding (7) and (8), we finally obtain

$$\frac{[f(c_2) - f(c_1)](1 - 2c_1)}{(c_2 - c_1)(1 - c_2 - c_1)} = 0$$

Possible solutions:

- $c_1 = 1/2$ – the point of maximum in $G(c)$ and an extraneous root.
- $f(c_1) = f(c_2)$ – a binodal, i.e., a boundary of the dome of the miscibility gap on the T - c diagram of the solid solution.

On the binodal:

$$\text{From (7) and (6): } \varphi(c_2) = [f(c_2) - f(c_1)] / (c_2 - c_1) = 0 = \varphi(c_1).$$

$$\text{From (5): } \partial G / \partial c = (G_A - G_B) + \varphi(c) = G_A - G_B.$$

Thus, Eqs. (2) and (3) of the common tangent line turn into

$$\begin{cases} \frac{\partial(\Delta G_{\text{mix}})}{\partial c} = \varphi(c_1, T, P) = \varphi(c_2, T, P) = 0 \\ \frac{\partial G}{\partial c} = G_A(T, P) - G_B(T, P) \end{cases} \quad (9) \text{ and } (10)$$

This is the main result for two-phase equilibrium in the model with the mixing energy in the form of a two-well potential symmetric with respect to the replacement of c by $1-c$, or, which is the same, symmetric with respect to the point $c_{\text{cr}} = 1/2$. As seen from Eq. (9), the concentrations c_1 and c_2 of the phases inside the two-phase region are determined by positions of the minima on the concentration dependence $\Delta G_{\text{mix}}(c)$ at given T and P and are independent on G_A and G_B . In its turn, the function $\partial G / \partial c$, which determines the position of the phase transformation curve on the T - P diagram, does not depend on the concentration c and is solely determined by the thermodynamic properties of crystals of pure components A and B.

Interstitial solid solutions

To proceed from the solid substitutional solutions to interstitial hydrogen solutions, imagine that the interstitial solution is a substitutional solution of the components $A = \text{Me}$ and $B = \text{MeH}_z$, where $z = \text{const}$. Then the concentration c_z of 1 mol of this interstitial solution will be equal to

$$c_z = \frac{N_{\text{MeH}_z}}{N_{\text{MeH}_z} + N_{\text{Me}}} = \frac{N_{\text{H}}/z}{N_{\text{A}}}, \quad (11)$$

where N_{A} is the Avogadro number; N_{Me} and N_{MeH_z} are the numbers of “molecules” of the components, and N_{H} is the total number of hydrogen atoms in 1 mol of the solution. For $\partial G / \partial c_z$ this gives

$$\frac{\partial G}{\partial c_z} = \frac{\partial G}{\partial N_H} \cdot \frac{1}{\partial c_z / \partial N_H} = \frac{\partial G}{\partial N_H} \cdot z N_A = z \mu_H^{\text{sol}} \cdot N_A \quad (12)$$

where $\mu_H^{\text{sol}} = \partial G / \partial N_H$ is the chemical potential of hydrogen in solid solution.

Thermodynamic equilibrium between the hydrogen in a sample of the solid solution and in the gaseous hydrogen surrounding the sample is reached when

$$\frac{1}{2} \mu_{\text{H}_2}^{\text{gas}} = \mu_H^{\text{sol}},$$

where $\mu_{\text{H}_2}^{\text{gas}}$ is the chemical potential of molecular hydrogen. Multiplying both sides of this equation by $z N_A$ and using condition (10) of two-phase equilibrium, we obtain

$$\frac{z}{2} G_{\text{H}_2}^{\text{gas}} = \frac{\partial G}{\partial c_z} = G_{\text{MeHz}} - G_{\text{Me}},$$

wherefrom

$$G_{\text{Me}} + \frac{z}{2} G_{\text{H}_2}^{\text{gas}} = G_{\text{MeHz}}$$

This energy balance exactly corresponds to the reaction $\text{Me} + (z/2)\text{H}_2 = \text{MeHz}$, in which $z = \text{const}$.

Estimates of the deviation of the $\Delta G^0(T)$ and $\Delta G^0(1/T)/T$ dependences from linearity due to changes in ΔH^0 and ΔS^0 with increasing temperature

The T and P values in Eqs. (9) and (10) for the common tangent are points on the equilibrium line for the isomorphic transformation $\text{Me}_{1-y}\text{H}_y + \frac{1}{2}(x-y)\text{H}_2 = \text{Me}_{1-x}\text{H}_x$. The equilibrium line is distinguished by the condition $\Delta G = 0$ for the Gibbs energy of this transformation. The dependences of $\ln P$ vs. $1/T$ analyzed in the present work determine a completely different, standard Gibbs energy $\Delta G^0(T, P_0)$ referred to the pressure $P_0 = 1$ atm. Since at $T = \text{const}$, the differential

$$dG = -SdT + VdP = VdP \text{ and, therefore, } G(P) = G(P_0) + \int_{P_0}^P VdP,$$

then for each fixed temperature T and equilibrium transformation pressure $P(T)$, the standard Gibbs energy can be

calculated from the condition $\Delta G^0(P_0) + \int_{P_0}^P \Delta V dP = 0$, where

$\Delta V(T, P) = V_{\text{MeHz}}(T, P) - V_{\text{Me}}(T, P) - (z/2)V_{\text{H}_2}(T, P)$ is the change in the molar volume of the Me–H system. Correspondingly,

$$\Delta G^0 = \int_P^{P_0} \Delta V dP.$$

For transformations at low hydrogen pressures up to several tens of atmospheres and temperatures of the order of the room one and above, gaseous hydrogen is well described by the Clapeyron-Clausius equation $PV = \nu RT$, where ν is the number of moles, and the difference between the molar volumes of the hydride and metal is negligible compared to the volume of hydrogen $(z/2)V_{\text{H}_2}$. Under these conditions, with good accuracy

$$\Delta G^0(T, P_0) = -\frac{z}{2} \int_P^{P_0} V_{\text{H}_2} dP = \frac{z}{2} RT \int_{P_0}^P \frac{dP}{P} = \frac{z}{2} RT \ln(P/P_0)$$

and we arrive at the well-known Eq. (1). If $\Delta H^0(P_0)$ and $\Delta S^0(P_0)$ are independent of temperature, Eq. (1) gives a linear dependence $\ln P$ vs. $1/T$, and the equation $\Delta G^0(T) = \Delta H^0(T) - T \cdot \Delta S^0(T)$ gives a linear dependence ΔG^0 vs. T .

It is worth noting that models with temperature-independent values of ΔH^0 and ΔS^0 describe quite satisfactorily the lines of phase transformations at moderate temperatures in many metal alloys without light elements. For most metals and alloys, the Debye temperatures are in the range of 250–450 K, therefore their heat capacities $C_p \approx C_v$ are close to $3R$ per gram-atom already at room temperature in accordance with the Dulong and Petit rule. With the transformation $x\text{A} + y\text{B} = \text{A}_x\text{B}_y$, an increase in temperature from T_1 to T_2 leads

to an increase in enthalpy by $\delta H^0(T_2) = \int_{T_1}^{T_2} C_p dT$ and entropy by

$$\delta S^0(T_2) = \int_{T_1}^{T_2} \frac{C_p}{T} dT \text{ for each of the phases. For the enthalpy and}$$

entropy of the phase transformation, this gives

$$\delta(\Delta H^0(T_2)) = \int_{T_1}^{T_2} \Delta C_p dT \approx 0 \quad \text{and} \quad \delta(\Delta S^0(T_2)) = \int_{T_1}^{T_2} \frac{\Delta C_p}{T} dT \approx 0,$$

because

$\Delta C_p = (x+y)C_p^{\text{AxB}_y} - (x \cdot C_p^{\text{A}} + y \cdot C_p^{\text{B}}) \approx 3R \cdot [(x+y) - (x+y)] \approx 3R \cdot 0 = 0$. Heat capacities close to the sum of the heat capacities of the components have been observed in many alloys and compounds, and this has even been called the Neuman-Kopp rule [11].

According to the results of Section [Interstitial solid solutions](#), in the metal-hydrogen systems with a symmetric miscibility gap, the quantities $\Delta H^0(P_0)$ and $\Delta S^0(P_0)$ acquire a clear physical meaning as the differences in thermodynamic quantities for a hydride of a fixed composition MeHz , gaseous hydrogen in a fixed amount $(z/2)\text{H}_2$, and the parent metal Me without hydrogen. This made it possible for the first time to estimate the changes in $\Delta H^0(P_0)$ and $\Delta S^0(P_0)$ with increasing temperature and the contribution of these changes to the temperature dependence $\Delta G^0(T, P_0)$ for transformations between the phases of variable composition.

The Pd–H and Pd–D systems

The experimental values of the decomposition pressure of palladium hydrides and deuterides taken from the literature [1–3] are shown in Fig. 1a. The positions of the critical points from Ref. [4] are also added, and they are found to be in good agreement with the linearly extrapolated dependences of the decomposition pressures. The decomposition pressures were chosen for the analysis because in metal-hydrogen systems, these pressures are usually much closer to the equilibrium pressures than the pressures of hydride formation [1,12].

Fig. 5a shows the dependences $\Delta G^0/T = (zR/2)\ln(P/P_0)$ for the Pd–H and Pd–D systems calculated in accordance with

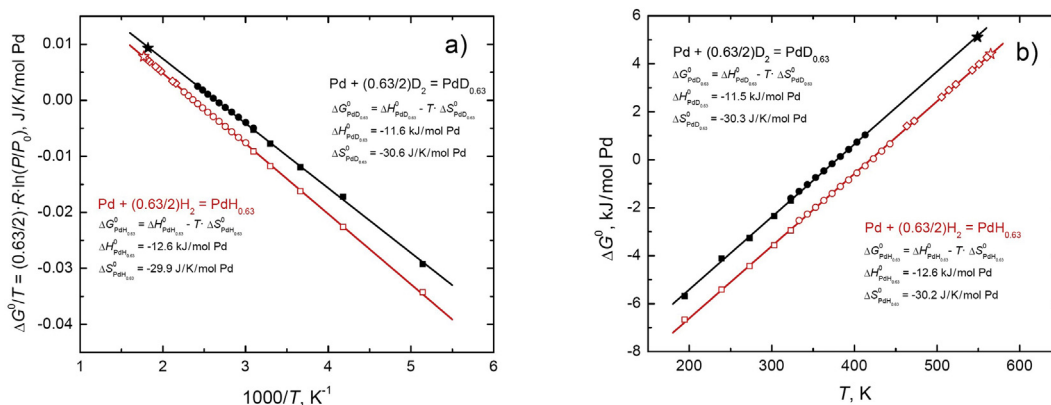


Fig. 5 – Experimental values of the standard Gibbs energy ΔG° for the reactions $\text{Pd} + (0.63/2)\text{H}_2 \rightarrow \text{PdH}_{0.63}$ (open red symbols) and $\text{Pd} + (0.63/2)\text{D}_2 \rightarrow \text{PdD}_{0.63}$ (solid black symbols) plotted as $\Delta G^\circ/T$ vs. $1/T$ (a) and ΔG° vs. T (b). Designations as in Fig. 1a. (For interpretation of the references to color in this figure legend, the reader is referred to the Web version of this article.)

Table 1 – Standard (at $P_0 = 1$ atm) enthalpy ΔH° and entropy ΔS° of formation of $\text{PdH}_{0.63}$ and $\text{PdD}_{0.63}$ calculated from the temperature dependences of the decomposition pressures of, respectively, palladium hydrides and deuterides measured in Refs. [1–3].

System	ΔH° , kJ/mol of $\text{PdH}_{0.63}$ or $\text{PdD}_{0.63}$	ΔS° , J/mol/K of $\text{PdH}_{0.63}$ or $\text{PdD}_{0.63}$	Reference and method
Pd–H	–12.6 (2)	–29.9 (4)	This paper, $\Delta G^\circ/T$ vs. $1/T$
	–12.6 (2)	–30.2 (4)	This paper, ΔG° vs. T
	–12.3 (1)	–28.7 (3)	Ref. [1], $\ln P$ vs. $1/T$
	–12.3 (2)	–29.1 (4)	Ref. [2], $\ln P$ vs. $1/T$
Pd–D	–11.6 (2)	–30.6 (4)	This paper, $\Delta G^\circ/T$ vs. $1/T$
	–11.5 (2)	–30.3 (4)	This paper, ΔG° vs. T
	–11.7 (1)	–30.8 (3)	Ref. [1], $\ln P$ vs. $1/T$
	–11.2 (2)	–29.4 (4)	Ref. [2], $\ln P$ vs. $1/T$

Eq. (1) using the experimental values of $\ln P$ vs. $1/T$ presented in Fig. 1a. A value of $z = 0.63$ was chosen for the calculations for both hydride and deuteride at $T = 0$ K, since the maximum values of z obtained at the lowest measurement temperature $T = 194.5$ K in Ref. [1] were $z = 0.635$ for the hydride and $z = 0.625$ for the deuteride. Fig. 5a also presents the values of the enthalpy ΔH° and entropy ΔS° of formation of the $\text{PdH}_{0.63}$ and $\text{PdD}_{0.63}$ phases obtained by linear interpolation of the experimental dependences $\Delta G^\circ/T$ vs. $1/T$.

Generally speaking, interpolation of experimental data as a function of reciprocal temperature is not the most accurate method to obtain any thermodynamic values, since this procedure greatly overestimates the statistical weight of the experimental points obtained at low temperatures – under

the conditions most difficult to achieve thermodynamic equilibrium. In this regard, we have also prepared Fig. 5b with the dependences $\Delta G^\circ(T)$, which should be linear as well and more suitable for precise interpolation.

Table 1 compares the values of ΔH° and ΔS° obtained in this paper and in Refs. [1,2]. Along with the experimental results from Refs. [1,2], the datasets analyzed in this paper include results for the near-critical region in the Pd–H system [3] and the positions of the critical points in both Pd–H and Pd–D systems [4]. The values of ΔH° and ΔS° presented in Refs. [1,2] were recalculated for the compositions $\text{PdH}_{0.63}$ and $\text{PdD}_{0.63}$. As seen from Table 1, the values obtained in our paper well agree with those from Refs. [1,2]. This suggests that the high-temperature points from Refs. [3,4] fall onto almost the same linear dependences as the low-temperature points considered previously [1,2].

To assess the changes $\delta H^\circ(T)$ and $\delta S^\circ(T)$ occurring in $\Delta H^\circ(T)$ and $\Delta S^\circ(T)$ with an increase in temperature from the minimum experimental value T_{\min} to the temperature T_{cr} of the critical point, we used the previously published temperature dependences of the heat capacity of the phases participating in the reactions $\text{Pd} + (z/2)\text{H}_2 = \text{PdH}_z$ and $\text{Pd} + (z/2)\text{D}_2 = \text{PdD}_z$ at $z = 0.63$. The results are shown in Fig. 6.

The heat capacities C_p of molecular hydrogen (blue curve in Fig. 6a) and deuterium (magenta curve in Fig. 6b) weakly depend on temperature and are approximately equal to $(7/2)R$, because in the temperature range shown on the figures, all rotational modes of H_2 and D_2 molecules are already excited, and the temperature is not high enough to excite a noticeable number of stretching modes. The differences δC in the heat capacities that determine the changes in $\Delta H^\circ(T)$ and $\Delta S^\circ(T)$ with increasing temperature are shown at the bottom of Fig. 6a and b with thick cyan lines. In contrast to what is observed in the formation of substitutional alloys without light elements (see Section Estimates of the deviation of the $\Delta G^\circ(T)$ and $\Delta G^\circ(1/T)/T$ dependences from linearity due to changes in ΔH° and ΔS° with increasing temperature), this differences are by no means negligible in comparison with the heat capacities of the components of the reactions.

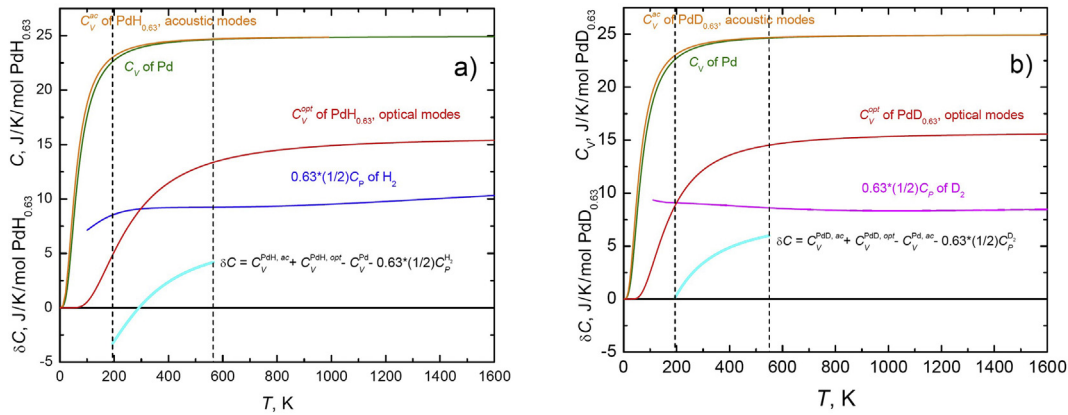


Fig. 6 – Heat capacities of the phases participating in the reactions $\text{Pd} + (0.63/2)\text{H}_2 = \text{PdH}_{0.63}$ (a) and $\text{Pd} + (0.63/2)\text{D}_2 = \text{PdD}_{0.63}$ (b). The C_p values for gaseous H_2 (blue curve) at $T \geq 298$ K are taken from Ref. [13] and at $T < 298$ K from Ref. [14]. The C_p values for D_2 (magenta curve) at $T \geq 298$ K are from Ref. [15] and at $T < 298$ K from Ref. [16]. Heat capacity C_V for Pd (olive curve) is calculated from its Debye temperature $\theta = 275$ K at $T = 298$ K [17]. Heat capacities C_V for acoustic modes (orange curve) and optical modes (red curve) in $\text{PdH}_{0.63}$ (a) and $\text{PdD}_{0.63}$ (b) are from Ref. [18]. The thick cyan curve shows the calculated difference in the heat capacities, which determines the changes $\delta H^0(T)$ and $\delta S^0(T)$ occurring in $\Delta H^0(T)$ and $\Delta S^0(T)$ with increasing temperature. The dashed vertical lines indicate the temperature ranges 194.5–565 K (a) and 194.5–549 K (b), in which the decomposition pressures of, respectively, palladium hydrides and deuterides were experimentally determined. (For interpretation of the references to color in this figure legend, the reader is referred to the Web version of this article.)

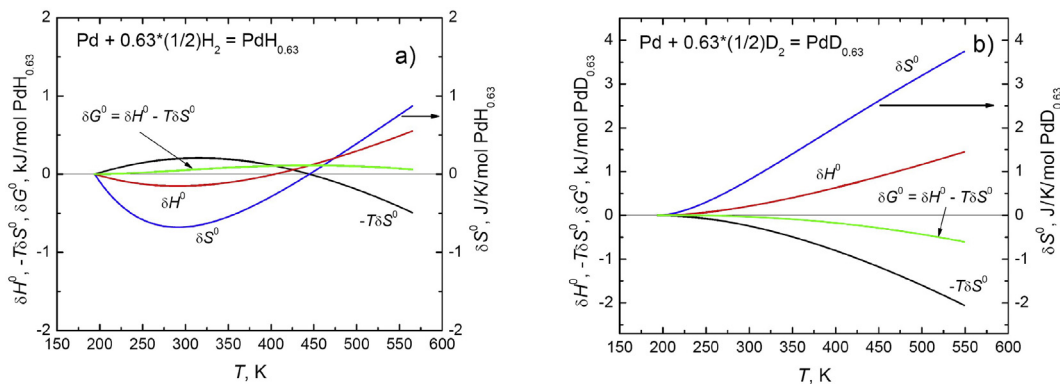


Fig. 7 – Temperature changes in the standard enthalpy (red curve); entropy (blue curve, right vertical scale); Gibbs energy (green curve), and the $-T \cdot \delta S^0(T)$ term of the Gibbs energy (black curve) for the reactions $\text{Pd} + (0.63/2)\text{H}_2 = \text{PdH}_{0.63}$ (a) and $\text{Pd} + (0.63/2)\text{D}_2 = \text{PdD}_{0.63}$ (b). (For interpretation of the references to color in this figure legend, the reader is referred to the Web version of this article.)

Fig. 7 shows temperature-induced variations in the stan-

dard enthalpy $\delta H^0(T) = \int_{T_{\min}}^T \delta C(T) \cdot dT$, entropy $\delta S^0(T) = \int_{T_{\min}}^T \frac{\delta C_p}{T} dT$, Gibbs energy $\delta G^0(T) = \delta H^0(T) - T \cdot \delta S^0(T)$ and, separately, in the $-T \cdot \delta S^0(T)$ term of the Gibbs energy for the reactions $\text{Pd} + (0.63/2)\text{H}_2 = \text{PdH}_{0.63}$ and $\text{Pd} + (0.63/2)\text{D}_2 = \text{PdD}_{0.63}$. $T_{\min} = 194.5$ K is the minimum temperature at which the decomposition pressures of palladium hydrides and deuterides were experimentally determined. The resulting dependences $\Delta G^0(1/T)/T - \delta G^0(1/T)/T$ and $\Delta G^0(T) - \delta G^0(T)$ are shown in Fig. 8.

The total changes accumulated in going from T_{\min} to T_{cr} are not very large, but noticeable. For example, in the Pd-D

system, ΔH^0 and ΔS^0 change by about 12%, and ΔG^0 changes by about 6%. The change in ΔG^0 is approximately two times less, because δH^0 and δS^0 have the same sign and the terms δH^0 and $-T \cdot \delta S^0$ in δG^0 partially compensate each other. In the Pd-H system, the compensation is more perfect: ΔH^0 changes by 4%, ΔS^0 by 3%, while the change in ΔG^0 is a few times less and only reaches 0.6%. As seen from Fig. 8a, the dependence $\Delta G^0(T) - \delta G^0(T)$ is well approximated by a straight line in the Pd-H system and satisfactorily in the Pd-D system. Fig. 8b shows that the dependences $\Delta G^0(1/T)/T - \delta G^0(1/T)/T$ are linear with good accuracy in both systems.

The Ni-H and Ni-D systems

Phase transformations in the Ni-H and Ni-D systems occur at pressures of the order of 1 GPa, when hydrogen can no longer

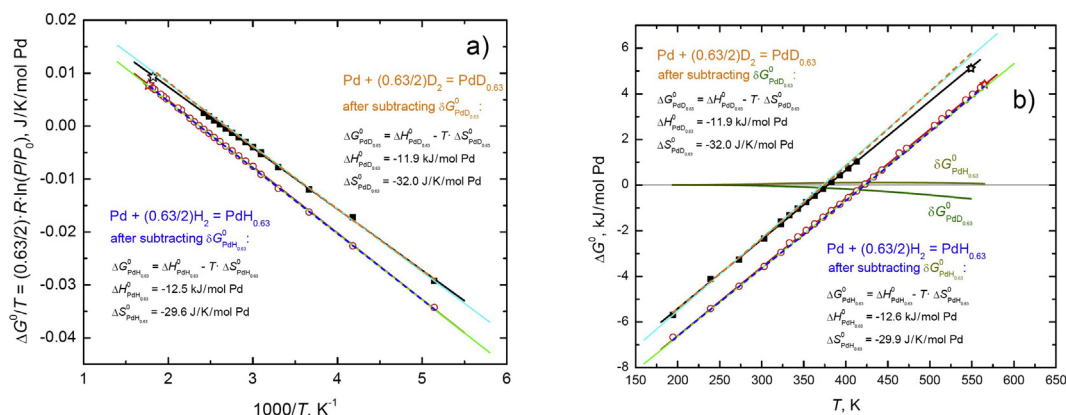


Fig. 8 – Copies of Fig. 5a and b with additional dependences shown by thick dashed lines and obtained by subtracting the calculated dependences $\delta G^0(1/T)/T$ (a) and $\delta G^0(T)$ (b). The dependences $\delta G^0(T)$ for the reactions $\text{Pd} + (0.63/2)\text{H}_2 = \text{PdH}_{0.63}$ and $\text{Pd} + (0.63/2)\text{D}_2 = \text{PdD}_{0.63}$ are depicted with green curves in Fig. 6a and b, respectively. The dashed curves demonstrate what the $\Delta G^0(1/T)/T$ and $\Delta G^0(T)$ dependences would look like if ΔH^0 and ΔS^0 were constants. These dependences are also approximated with thin straight lines. (For interpretation of the references to color in this figure legend, the reader is referred to the Web version of this article.)

be considered an ideal gas, and its molar volume decreases to such an extent that, compared with it, the differences in the molar volumes of solid phases cannot be neglected. Accordingly, when calculating the standard (at $P_0 = 1$ atm) Gibbs

energy from the condition $\Delta G^0(P_0) + \int_{P_0}^P \Delta V dP = 0$, the differ-

ence $\Delta V(T,P) = V_{\text{MeH}_2}(T,P) - V_{\text{Me}}(T,P) - (z/2)V_{\text{H}_2}(T,P)$ significantly differs from $(z/2)V_{\text{H}_2}(T,P)$, and $V_{\text{H}_2}(T,P)$ is much larger than the volume of an ideal gas. Compared to the Pd–H and Pd–D systems, the factor z drops out of the formulas for the Ni–H and Ni–D systems, since the compositions of nickel hydrides and deuterides are close to NiH and NiD at $T \rightarrow 0$ K (see Fig. 3b).

In addition, the mixing energy $\Delta G_{\text{mix}}(T,P,c)$ of solid solutions considered in Section Thermodynamics of solid solutions with a symmetric energy of mixing is a function of pressure. Decomposition of hydrides and deuterides of palladium occurs at pressures of the first tens of atmospheres, and its effect on ΔG_{mix} is negligible. In the Ni–H and Ni–D systems, the pressure of the isomorphic phase transformation is not small, but its effect on ΔG_{mix} can also be neglected, since, as has been shown in Ref. [19] and confirmed in Ref. [10], solid nickel-hydrogen solutions well obey the Vegard law and their molar volume v varies linearly over the entire concentration range $0 \leq x \leq 1$. Accordingly, when the solution is separated into phases with different hydrogen concentrations, the volume of the sample does not change and, therefore, its ΔG_{mix} does not change either, since $d(\Delta G_{\text{mix}}) = \Delta v \cdot dP$ at a constant temperature. Thus, on the T - x phase diagram of metastable Ni–H solutions at $P_0 = 1$ atm, the critical temperature and boundary concentrations of the miscibility gap will be the same as at the equilibrium high pressures.

Taking into account all the above, temperature dependences of the standard Gibbs energy $\Delta G^0(T)$ of hydride (deuteride) formation in the Ni–H and Ni–D systems were

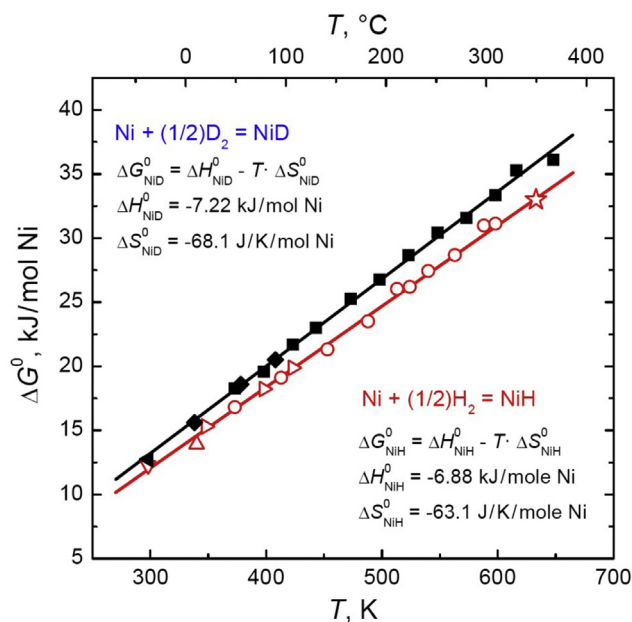


Fig. 9 – Experimental values of the standard Gibbs energy ΔG^0 for the reactions $\text{Ni} + (1/2)\text{H}_2 \rightarrow \text{NiH}$ (open red symbols) and $\text{Ni} + (1/2)\text{D}_2 \rightarrow \text{NiD}$ (solid black symbols) plotted as a function of temperature [9]. (For interpretation of the references to color in this figure legend, the reader is referred to the Web version of this article.)

calculated in Ref. [9]. These dependences and the values of ΔH^0 and ΔS^0 obtained by their linear interpolation are shown in Fig. 9. The dependences of $\Delta G^0/T$ vs. $1/T$ shown in Fig. 3a are recalculated from the experimental data presented in Fig. 9. As seen from Figs. 3a and 9, the dependences of both types are linear with good accuracy. The parameters ΔH^0 and ΔS^0 of the linear fit indicated in Fig. 9 are preferable. No critical point is indicated on the dependencies for the Ni–D system, since its position has not yet been determined.

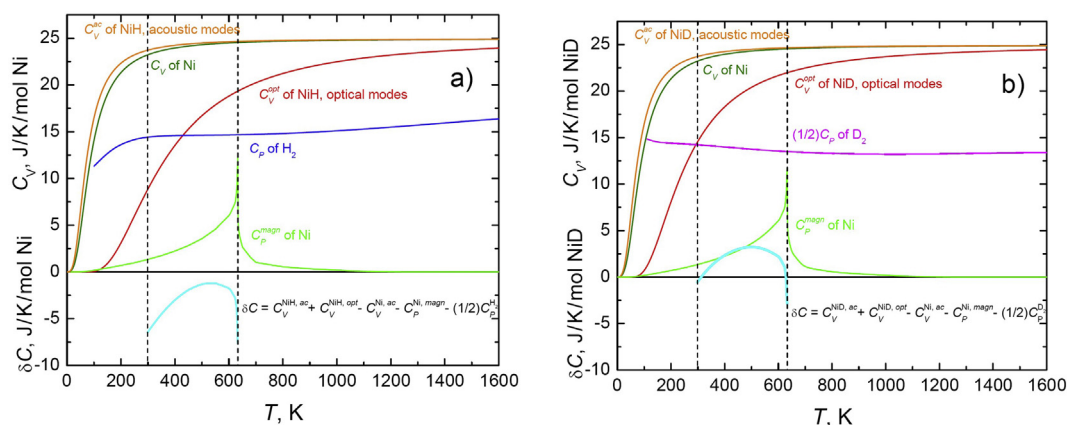


Fig. 10 – Heat capacities of the components of the reactions $\text{Ni} + (1/2)\text{H}_2 \rightarrow \text{NiH}$ (a) and $\text{Ni} + (1/2)\text{D}_2 \rightarrow \text{NiD}$ (b). The $C_p(T)$ dependences for gaseous H_2 (blue curve) and D_2 (magenta curve) are the same as in Fig. 6a and b, respectively. The heat capacities C_V for Ni (olive curves) and for acoustic modes in NiH and NiD (orange curves) are calculated from their Debye temperatures $\theta_{\text{Ni}} = 360$ K and $\theta_{\text{NiH}} = 300$ K determined in Ref. [22]. Heat capacities C_V for optical modes (red curves) in NiH (a) and NiD (b) are from Ref. [18]. The magnetic contribution to the heat capacity of Ni (green curves) is taken from Ref. [20]. The thick cyan curves show the difference in the heat capacities, which determines the changes $\delta H^0(T)$ and $\delta S^0(T)$ occurring in $\Delta H^0(T)$ and $\Delta S^0(T)$ with increasing temperature. The dashed vertical black lines indicate the temperature range 298–633 K, in which the decomposition pressures of nickel hydrides and deuterides were measured [9]. (For interpretation of the references to color in this figure legend, the reader is referred to the Web version of this article.)

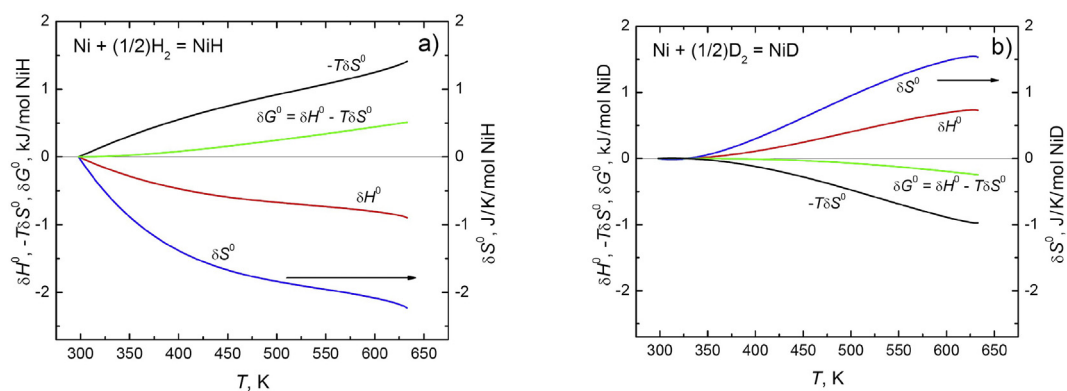


Fig. 11 – Temperature changes in the standard enthalpy (red curve); entropy (blue curve, right vertical scale); Gibbs energy (green curve), and the $-T \cdot \delta S^0(T)$ term of the Gibbs energy (black curve) for the reactions $\text{Ni} + (1/2)\text{H}_2 = \text{NiH}$ (a) and $\text{Ni} + (1/2)\text{D}_2 = \text{NiD}$ (b). (For interpretation of the references to color in this figure legend, the reader is referred to the Web version of this article.)

The temperature dependences of the heat capacities of the phases involved in the reactions $\text{Ni} + (1/2)\text{H}_2 \rightarrow \text{NiH}$ and $\text{Ni} + (1/2)\text{D}_2 \rightarrow \text{NiD}$ are presented in Fig. 10. Unlike palladium, nickel is a ferromagnet, and the magnetic contribution to its heat capacity [20] is shown in Fig. 10a and b by the green curves. Nickel hydride remains paramagnetic at temperatures down to 0.3 K [21]. Consequently, there is no magnetic contribution to its heat capacity in the investigated temperature range above 298 K.

Fig. 11 shows temperature dependences $\delta H^0(T)$, $\delta S^0(T)$, $\delta G^0(T)$, and $-T\delta S^0(T)$ for the Ni–H and Ni–D systems, calculated by the same formulas as for the Pd–H and Pd–D systems (see Section The Pd–H and Pd–D systems) using the $\delta C(T)$ dependences plotted with thick cyan curves at the bottom of

Fig. 10a and b, respectively. The resulting dependences $\Delta G^0(T) - \delta G^0(T)$ are plotted with thick dashed curves in Fig. 12.

Similar to what we observed in the Pd–H and Pd–D systems, the terms δH^0 and $-T \cdot \delta S^0$ significantly compensate each other in δG^0 of the Ni–H and Ni–D systems. For example, as seen from Fig. 10a, the value of $\delta G^0 \approx 0.5$ kJ/mol NiH in the Ni–H system at the maximum temperature $T_{\text{cr}} = 633$ K turns out to be approximately two times less than $|\delta H^0|$ and three times less than $|-T \cdot \delta S^0|$. Compared to the total change in $\Delta G^0(T)$ upon heating from 298 to 633 K, this δG^0 contributes less than 3% and only leads to a negligibly small deviation of the $\Delta G^0(T) - \delta G^0(T)$ dependence from the linearity (see the dashed blue line in Fig. 12). The linearity of the $\Delta G^0(T) - \delta G^0(T)$ dependence in the Ni–D system

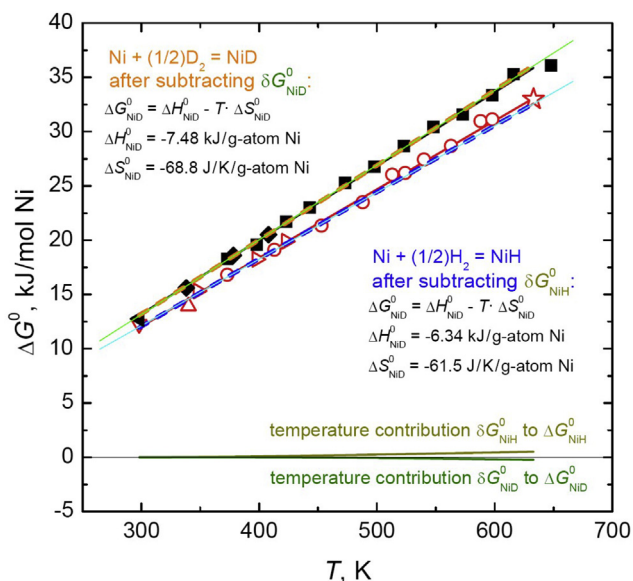


Fig. 12 – A copy of Fig. 9 with additional dependences shown by thick dashed lines and obtained by subtracting the calculated dependences $\delta G^0(T)$, which are depicted with green curves in Fig. 10a and b and reproduced at the bottom of this figure. The dashed curves demonstrate what the $\Delta G^0(T)$ dependences would look like if ΔH^0 and ΔS^0 were constants. To illustrate the linearity of these dependences, they are also approximated with thin straight lines. (For interpretation of the references to color in this figure legend, the reader is referred to the Web version of this article.)

(dashed orange line in Fig. 12) is even better, since the contribution from δG^0 at 633 K does not exceed 1.5%.

Conclusions

The work was devoted to one of the puzzling problems of hydrogen materials science, which could not find a solution for several decades. The problem was that in one of the most important metal-hydrogen systems, the palladium-hydrogen system, the logarithm of the hydride formation pressure linearly depends on the reciprocal temperature over the entire investigated temperature range. Since this logarithm is proportional to the standard Gibbs energy $\Delta G^0 = \Delta H^0 - T \cdot \Delta S^0$ of hydride formation divided by temperature, it was assumed that the standard enthalpy ΔH^0 and entropy ΔS^0 of the reaction remain constant all along the investigated section of the equilibrium line. This was surprising, since palladium hydride does not have a fixed composition and is formed via a transition between two isomorphous phases of the Pd–H solid solution with the hydrogen concentrations approaching each other with increasing temperature and coinciding at the critical point, where the transition line breaks off. Attempts to disclose the specific features of the Pd–H system that

maintain the constancy of ΔH^0 along the transition line have not been successful until recently.

This paper showed that the main feature of the Pd–H system, which ensures the linearity of the $\Delta G^0/T$ vs. $1/T$ dependence, consists in the symmetry of the miscibility gap in the solid Pd–H solutions with respect to the concentration $z/2$, where z is the maximum H-to-metal atomic ratio attained by the hydride in equilibrium with Pd metal at $T \rightarrow 0$ K. A simple thermodynamic analysis showed that a model with the mixing energy ΔG_{mix} in the form of a double-well potential symmetric relative to $z/2$ gives a symmetric miscibility gap in the interstitial solution and makes it possible to determine the line of the corresponding isomorphous transition using only the properties of the pure metal and its hydride with a fixed hydrogen content z .

Switching from the problem with variable phase compositions to the problem with fixed compositions opened the possibility to establish the presence and magnitude of changes in ΔH^0 and ΔS^0 for the reactions of hydride formation in metal-hydrogen systems with solid solutions. Using the literature data for the metal and the hydride with the maximum hydrogen content z , we calculated the temperature dependences of changes in ΔH^0 , ΔS^0 , and ΔG^0 for the Pd–H and Pd–D systems, and also for the analog systems Ni–H and Ni–D. The calculations showed that the total changes accumulated in both ΔH^0 and ΔS^0 in going from the minimum measurement temperature to the critical temperature vary from 12% for the Pd–D system down to 4% in the Pd–H system. The changes δH^0 and δS^0 in ΔH^0 and ΔS^0 are mostly of the same sign, and the terms δH^0 and $-T \cdot \delta S^0$ partially compensate each other in δG^0 . As a consequence, the changes in ΔG^0 are two to five times less than the changes in ΔH^0 and ΔS^0 and reach 6% in the Pd–D system and 0.6% in the Pd–H system. The resulting deviations of the $\Delta G^0/T$ vs. $1/T$ and G^0 vs. T dependences from linearity lie within the experimental error and can only manifest themselves in slight changes in the values of ΔH^0 and ΔS^0 obtained by approximating these dependences by straight lines.

Palladium and its alloys are widely used for purification of hydrogen, as well as catalysts that promote the hydrogen absorption and desorption by other metals and alloys, and also as hydrogen sensors, etc. As was noted many years ago [4], much fundamental knowledge was gained and a lot of experimental techniques were developed in the investigation of the Pd–H system and later implemented in the study of other, more complex systems important for applications. Nevertheless, despite a great deal of experimental and theoretical work on palladium hydrides published since then, some unusual experimental findings in the Pd–H system itself have not yet been understood. For example, after about 50 years of studying the inverse isotope effect in the superconductivity of the Pd–H/D system [23], which strikingly contradicts the Bardeen-Cooper-Schrieffer (BCS) theory [24], neutron spectroscopy [25] has shown the fallacy of the conventional explanation [26], relating this effect to the strong anharmonicity of optical vibrations of hydrogen atoms in palladium hydride. We believe that thanks to the

present paper, the number of unexplained phenomena in the Pd–H system has become one less.

Declaration of competing interest

The authors declare that they have no known competing financial interests or personal relationships that could have appeared to influence the work reported in this paper.

Acknowledgements

The work was partly supported by the Russian Foundation for Basic Research [grant No. 20-02-00638]. The authors are grateful to Dr. R.Kh. Azimov for valuable help and recommendations.

REFERENCES

- [1] Wicke E, Nernst GH. Zustandsdiagramm und thermodynamisches Verhalten der Systeme Pd/H₂ und Pd/D₂ bei normalen Temperaturen; H/D-Trenneffekte. *Ber Bunsenges Phys Chem* 1964;68:224–35.
- [2] Lässer R, Klatt K-H. Solubility of hydrogen isotopes in palladium. *Phys Rev B* 1983;28:748–58. <https://doi.org/10.1103/PhysRevB.28.748>.
- [3] Wicke E, Blaurock J. Equilibrium and susceptibility behaviour of the Pd/H₂ system in the critical and supercritical region. *Ber Bunsenges Phys Chem* 1981;85:1091–6. <https://doi.org/10.1002/bbpc.19810851203>.
- [4] Wicke E, Brodowsky H. Hydrogen in palladium and palladium alloys. In: Allefeld G, Vökl J, editors. *Hydrogen in metals II, topics in appl. Physics*. vol. 29. Berlin, Heidelberg, New York: Springer-Verlag; 1978. p. 73–155.
- [5] Joubert J-M, Thiébaud S. Thermodynamic assessment of the Pd–H–D–T system. *J Nucl Mater* 2009;395:79–88. <https://doi.org/10.1016/j.jnucmat.2009.09.021>.
- [6] Speicer R. The thermodynamics of metal-hydrogen systems. In: Mueller W, Blackledge JP, Llbowitz GG, editors. *Metal hydrides*. New York: Academic Press; 1968. p. 51–89 [Chapter 3].
- [7] Flanagan TB, Lynch JF. Thermodynamics of a gas in equilibrium with two nonstoichiometric condensed phases. Application to metal/hydrogen systems. *J Phys Chem* 1975;79:444–8. <https://doi.org/10.1021/J100572A010>.
- [8] Pryde JA, Titcomb CG. Solution of hydrogen in niobium. *Trans Faraday Soc* 1969;65:2758–65. <https://doi.org/10.1039/TF9696502758>.
- [9] Antonov VE, Ivanov AS, Kuzovnikov MA, Tkacz M. Neutron spectroscopy of nickel deuteride. *J Alloys Compd* 2013;580:S109–13. <https://doi.org/10.1016/j.jallcom.2013.03.021>.
- [10] Fukai Y, Yamatomo S, Harada S, Kanazawa M. The phase diagram of the Ni–H system revisited. *J Alloys Compd* 2004;372:L4–5. <https://doi.org/10.1016/j.jallcom.2003.09.134>.
- [11] Swalin RA. *Thermodynamics of solids*. New York: John Wiley & Sons; 1962.
- [12] Antonov VE, Latynin AI, Tkacz M. T–P phase diagrams and isotope effects in the Mo–H/D systems. *J Phys Condens Matter* 2004;16:8387–98. <https://doi.org/10.1088/0953-8984/16/46/024>.
- [13] NIST Standard Reference Database 69: NIST Chemistry WebBook. <https://webbook.nist.gov/cgi/cbook.cgi?ID=C1333740&Mask=1&Type=JANAFG&Plot=on>.
- [14] Stewart RB, Roder HM. Properties of normal and parahydrogen. In: *Technology and uses of liquid hydrogen*. New York: Pergamon Press; 1964. p. 379–404 [Chapter 11].
- [15] NIST Standard Reference Database 69: NIST Chemistry WebBook. <https://webbook.nist.gov/cgi/cbook.cgi?ID=C7782390&Mask=1#Thermo-Gas>.
- [16] Richardson IA, Leachman JW, Lemmon EW. Fundamental equation of state for deuterium. *J Phys Chem Ref Data* 2014;43:013103. <https://doi.org/10.1063/1.4864752>.
- [17] KnowledgeDoor. http://www.knowledgedoor.com/2/elements_handbook/debye_temperature.html.
- [18] Antonov VE, Fedotov VK, Ivanov AS, Kolesnikov AI, Kuzovnikov MA, Tkacz M, Yartys VA. Lattice dynamics of high-pressure hydrides studied by inelastic neutron scattering. *J Alloys Compd* 2022;905:164208. <https://doi.org/10.1016/j.jallcom.2022.164208>.
- [19] Antonov VE, Baier M, Dorner B, Fedotov VK, Grosse G, Kolesnikov AI, Ponyatovsky EG, Schneider G, Wagner FE. High-pressure hydrides of iron and its alloys. *J Phys Condens Matter* 2002;14:6427–45. <https://doi.org/10.1088/0953-8984/14/25/311>.
- [20] Meschter PJ, Wright JW, Brooks CR, Kollie TG. Physical contributions to the heat capacity of nickel. *Phys Chem Solids* 1981;42:861–71. [https://doi.org/10.1016/0022-3697\(81\)90174-8](https://doi.org/10.1016/0022-3697(81)90174-8).
- [21] Antonov VE, Belash IT, Zharikov OV, Palnichenko AV. A study on superconductivities of high pressure phases in the Re–H, Ru–H, Rh–H, and Ni–H systems. *Phys Status Solidi* 1987;142:K155–99. <https://doi.org/10.1002/psb.2221420246>.
- [22] Kolesnikov AI, Natkaniec I, Antonov VE, Belash IT, Fedotov VK, Krawczyk J, Mayer J, Ponyatovsky EG. Neutron spectroscopy of MnH_{0.86}, NiH_{1.05}, PdH_{0.99} and harmonic behaviour of their optical phonons. *Physica B* 1991;174:257–61. [https://doi.org/10.1016/0921-4526\(91\)90616-M](https://doi.org/10.1016/0921-4526(91)90616-M).
- [23] Stritzker B, Buckel W. Superconductivity in the palladium-hydrogen and the palladium-deuterium systems. *Z Phys* 1972;257:1–8. <https://doi.org/10.1007/BF01398191>.
- [24] Bardeen J, Cooper LN, Schrieffer JR. Theory of superconductivity. *Phys Rev* 1957;108:1175–204. <https://doi.org/10.1103/PhysRev.108.1175>.
- [25] Kuzovnikov MA, Antonov VE, Hansen T, Ivanov AS, Kolesnikov AI, Kulakov VI, Muzalevsky VD, Savvin S, Tkacz M. Isotopic dependence of the frequency of optical vibrations in molybdenum monohydride. *J Alloys Compd* 2022;893:162299. <https://doi.org/10.1016/j.jallcom.2021.162299>.
- [26] Errea I, Calandra M, Mauri F. First-principles theory of anharmonicity and the inverse isotope effect in superconducting palladium-hydride compounds. *Phys Rev Lett* 2013;111:177002. <https://doi.org/10.1103/PhysRevLett.111.177002>.